ISBN: 978-3-95450-234-9 ISSN: 2673-5504 doi:10.18429/JACoW-SRF2023-WEPWB073

PROTOTYPE HB650 CRYOMODULE HEAT LOADS SIMULATIONS*

G. Coladonato[1,†], D. Passarelli, V. Roger, Fermilab, Batavia, IL, USA
[1]also at University of Illinois, Chicago, IL, USA

Abstract

During the design stages of the PIP-II cryomodules, many analytical calculations and FEA have been performed on simpler geometry in order to estimate the heat loads and also to optimize the design. To better analyse the cryomodule cold tests, simulations have been performed with MATLAB to determine the temperature of the main components during cool-down and to determine the heat loads of the cryomodule. These simulations have been applied to the High Beta 650 MHz prototype cryomodule design and compared to the cold tests performed on it.

INTRODUCTION

Over the last years, calculations have been done to estimate the heat loads of the PIP-II linac [1] in order to design the appropriate cryogenic plant and the cryogenic distribution system. Therefore, accurate estimations of these heat loads are crucial for the project. In early 2023, the assembly of the prototype HB650 cryomodule was completed [2] and the cold tests started to evaluate its performance [3]. This cool-down and heat analysis gave us a great opportunity to compare the estimation to the measurements and also to develop with MATLAB a reliable tool to estimate the cooling time and heat loads in an automatic way. While previous studies have explored this aspect [4], the novelty lies in validating the results using actual data from experimental testing, further enhancing the reliability and applicability of the heat load calculations to use later on the LB650, SSR1 and SSR2 cryomodules [5, 6, 7].

CRYOMODULE DESIGN AND FIRST COOL-DOWN

The PIP-II SSR and 650 cryomodules are designed adopting the Fermilab style cryomodule that uses a room temperature strongback as foundation. This design choice is part of a design strategy [8] that was defined by the project to standardize parts in between cryomodules [9].

The Figure 1 describes the cryomodule layout of the HB650 cryomodule. A High Temperature Thermal shield (HTTS) to shield the heat loads by radiation from the vacuum vessel and to intercept heats by conduction on several components such as the support posts, couplers, relief line, pressure transducer lines, bayonets and cryogenic valves. A Low Temperature thermal source (LTTS) is being used as a thermal intercept for the beam line, couplers, relief line and support posts. A cool-down valve is used to cool-down the cavities up to 4 K, then an heat exchanger, Joule Thomson valve and pumping line are used together to reach 2 K.

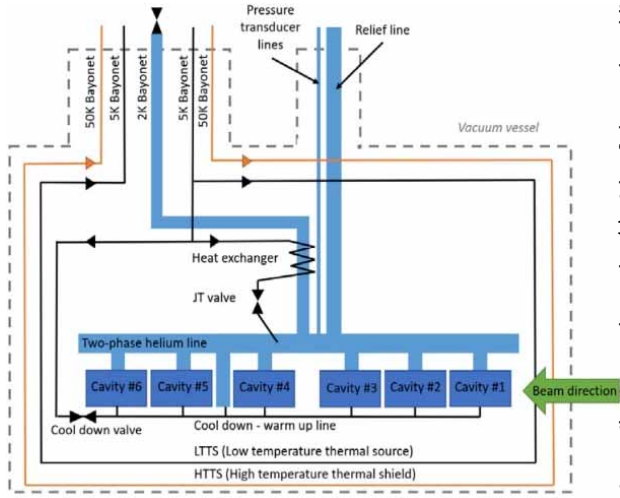

Figure 1: HB650 cryomodule layout.

The cool-down of the cryomodule is done using a detailed procedure to operate safely cryomodule and reach the appropriate performance. First only the thermal shield is cooled down from room temperature to 50 K by maintaining a maximum temperature difference of 100 K across the shield. While maintaining close the outlet of the LTTS and open the cool-down valve, the cavities are cooled to 4 K. The requirement is to go as fast as possible and to ensure a minimum rate of 20 K/hr between 175 K and 90 K. This step is critical to ensure a flux expulsion of the cavities required to reach a high Q_0. The next step is to open the outlet of the LTTS cooling down many thermal intercepts and reducing the 2 K heat loads. Finally, the cool-down valve is closed, and the Joule Thomson valve is open to reach 2 K.

This cryomodule being a prototype, it has been decided to close the helium inlets during the night for safety reasons. That is why the curves on the Figure 2 shows two plateaus. It took 49 hours to cool-down the thermal shield before starting to cool-down the cavities until 4 K and finally to reach 2 K.

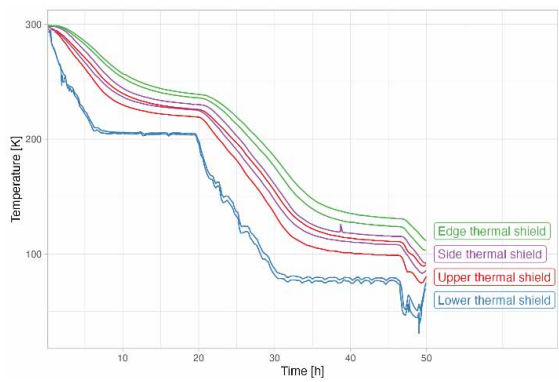

Figure 2: Cool-down of the HTTS.

* Work supported by Fermi Research Alliance, LLC under Contract No. DE AC02 07 CH11359 with the United States Department of Energy
† gcolad2@uic.edu

ISBN: 978-3-95450-234-9 ISSN: 2673-5504 doi:10.18429/JACoW-SRF2023-WEPWB073

VALIDATION OF THE MODEL

The Simulink/Simscape model offers a powerful tool for analyzing the thermal behavior of the HB650 cryomodule components. This model adopts a 0D approach, where each component is treated as a thermal mass. The focus is on considering the mass and specific heat of the components, as well as establishing thermal resistances to connect the components together.

The heat exchange between these components can occur through radiative or conductive mechanisms. To accurately calculate the thermal resistances, the model takes into account the geometry and the material conductivity at each interface. By integrating these factors, the model captures the overall thermal dynamics of the cryomodule system.

As a proof of concept, a first model has been developed considering the lower thermal shield (see Fig. 3) and the following interfaces. It is thermally linked to the side part of the thermal shield with thermal straps. The lower thermal shield is also cooled down by the extruded pipe operating at 50 K, as it is welded to the pipe. Moreover, the radiative exchange with the vacuum vessel has been considered.

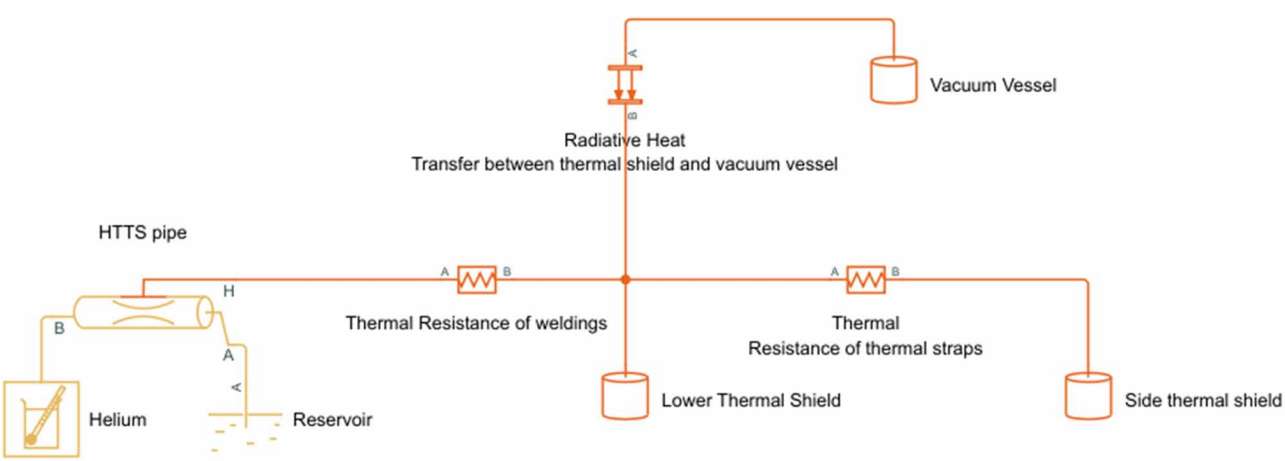

Figure 3: Simscape model of the lower thermal shield.

To validate the model, the inlet temperature of the extruded pipe (see Fig. 4) has been used. By comparing the temperature curves of each component from the model with the corresponding experimental data, the model's accuracy can be evaluated. It is important to note that the primary objective of this model is not to predict component temperature during transient states, as finite element analysis (FEA) models excel in that regard. Instead, the model serves to calculate the heat loads of each component, while the comparison between the model and experimental data verifies if these heat loads have been adequately considered.

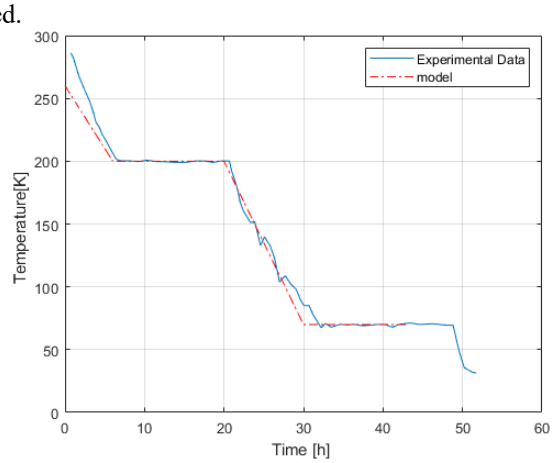

Figure 4: Inlet helium temperature.

Transient states are not the main focus of this model as they are better analyzed by FEA models. The 0D Simulink/Simscape model does not fully capture the complex temperature variations of each component. Nevertheless, by comparing the model to the experimental data under steady-state conditions, it becomes clear if the heat loads on the components have been properly accounted for.

HB650 PROTOTYPE CRYOMODULE MODEL

This cryomodule is a very complex system, composed of many parts for which the thermal links and masses need to be accounted properly into the model. For this reason, it was decided to divide the thermal shield into 4 different parts as described in the Figure 5.

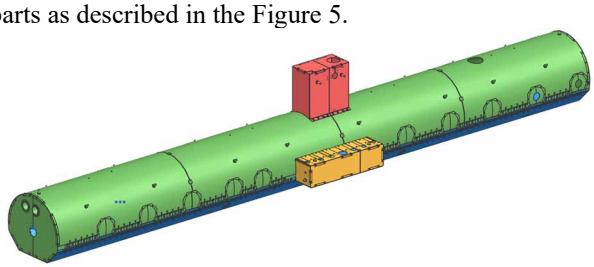

Figure 5: Thermal shield partitions considered in the model. In blue, the lower thermal shield, in green the upper thermal shield, in red the top part of the shield and in orange the side part of the shield.

ISBN: 978-3-95450-234-9 ISSN: 2673-5504 doi:10.18429/JACoW-SRF2023-WEPWB073

In the following chapters, the cool-down of the main cryomodule components will be compared to the model focusing on the initial phase of the cooling. This phase shows a slower rate, allowing for a more comprehensive analysis and comparison of the steady-state behaviour.

Lower Thermal Shield

The thermal shield of the HB650 cryomodule is used to reduce the heat loads by radiation received by the cavities. To avoid important temperature gradient in between the thermal shield parts, thermal straps have been connected. Nevertheless, the thermal resistance of these straps has been considered using this equation (1):

$$R = \frac{L}{Area \cdot \lambda(T)} , \quad (1)$$

where L is the length of the thermal strap's wires, Area is the area of contact between the component and the thermal strap, finally λ is the conductivity of copper.

The temperature data from TX061 and TX064 glued on the extruded pipe have been compared to the model prediction (see Fig. 6).

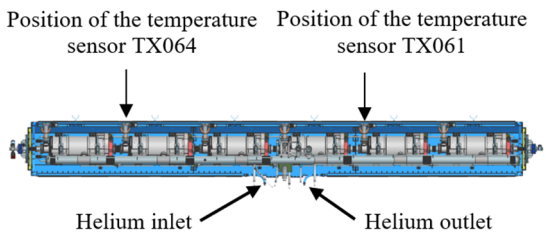

Figure 6: Temperature sensor positions on the lower thermal shield.

The results obtained for the lower thermal shield are shown in Fig. 7. Results from the model match the experimental data. The slight discrepancies can be attributed to the fact that the model uses an average temperature of the lower thermal shield.

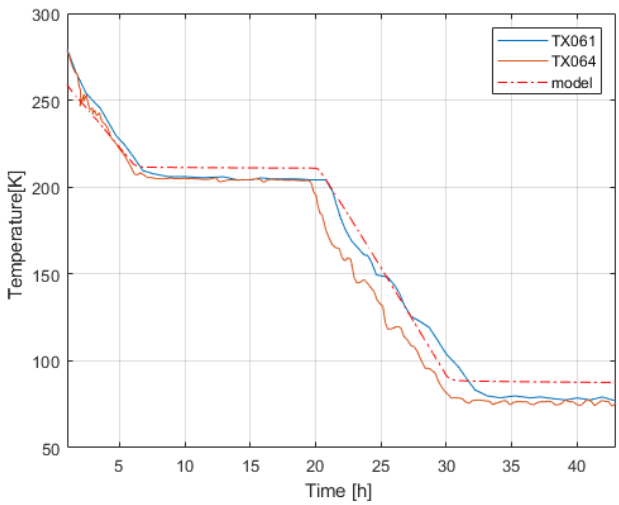

Figure 7: Lower thermal shield results.

Couplers

The modelling of the couplers in an 0D representation was one the most challenging part of this project due to the fact that the coupler temperature is not uniform. To address this challenge, it was necessary to divide the coupler into three distinct thermal masses. The first thermal mass corresponds to the ambient temperature, where the coupler is connected to the vacuum vessel. The second mass is the HTTS intercept, where the coupler is thermally linked to the HTTS with two thermal straps. The third mass is the LTTS intercept, where the coupler is thermally connected to the LTTS line using two other thermal straps. Each mass was connected by pipes, which were considered as two resistances in parallel. The copper layer inside the pipe contributed to one of the resistances, while the stainless-steel pipe formed the other. The length and contact area of the pipes were taken into account to calculate the respective resistances. Moreover, a resistance of niobium was considered between the last part of the coupler and the cavity, accounting for the thermal interaction between these components.

Figure 8 shows the location of the temperature sensors TX270 and TX271 on the coupler.

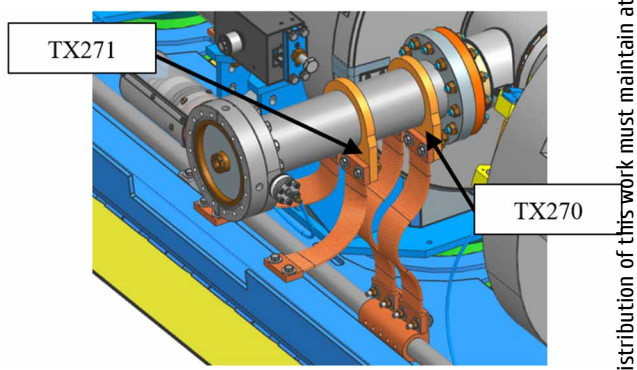

Figure 8: Temperature sensor positions on the coupler.

The observed discrepancy in Fig. 9 between the model and the actual data can be attributed to the complex structure of the couplers, which add challenges to estimate accurately the heat transfers. Additionally, the significant temperature difference between the two intercepts further contributes to the variation between the model and the experimental data.

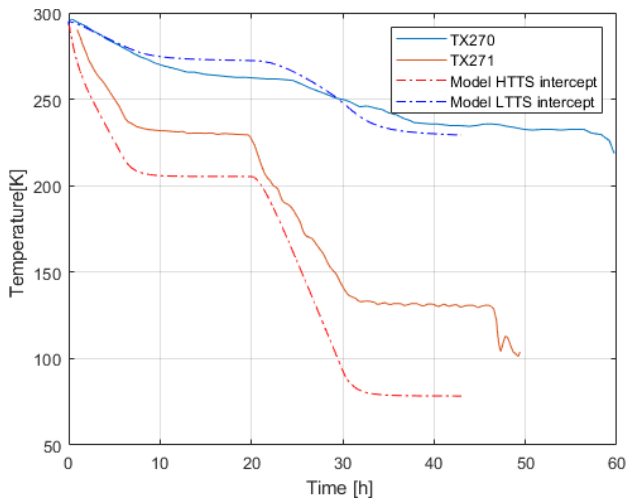

Figure 9: Coupler results.

ISBN: 978-3-95450-234-9 ISSN: 2673-5504 doi:10.18429/JACoW-SRF2023-WEPWB073

G11 Support Posts, Cavity Supports, and Cavities

The G11 support posts (see Fig. 10) are critical assemblies of the coldmass as they ensure its structural stability and also its insulation from the room temperature strongback. These posts have heat transfers with the strongback and the HTTS with two thermal straps. Each titanium cavity support (see Fig. 10), positioned on top of the G11 support posts, has two thermal straps connected to the LTTS pipe. Additionally, the radiation from the cavity support to the cavities has been considered.

The cavities, located in the middle of the coldmass, are cooled down by the cool-down line. Each cavity is indirectly connected to a coupler through a niobium pipe, serving as a thermal resistance. Moreover, the radiation from the HTTS to the cavities has been considered. Based on the design of the interface in between the cavity support and the cavity [2], it has been decided to consider that there was no heat-exchange in between these parts.

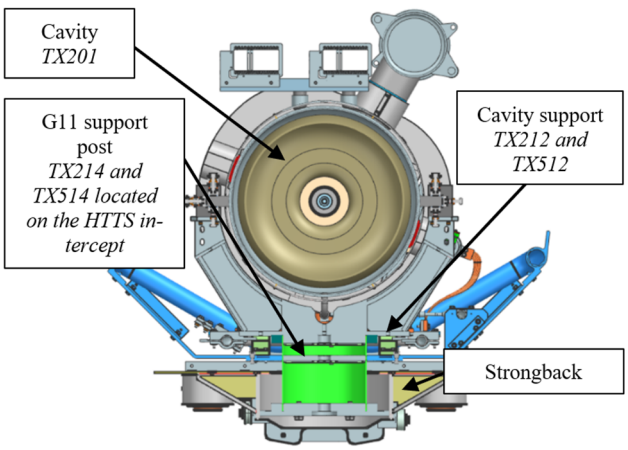

Figure 10: Cross section of the beam line with the strongback assembly.

The results obtained for the G11 supports posts, cavity supports and cavity are shown in Figs. 11, 12, and 13. For these three components, the model matches the experimental data. The comparison of the cavity cool down curves in Fig. 13 gives good confidence that the heat loads have been properly modelled.

HEAT LOADS RESULTS

The heat loads have been calculated with the Simulink/Simscape model using the Equation (2) once the cool-down was completed with the cavities at 2 K.

$$Q = \frac{\Delta T}{R}, \qquad (2)$$

where ΔT is the temperature difference and R the thermal resistance.

The results of the heat load analysis on the HTTS show some differences compared to previous studies. This disparity comes from the improved calculation of radiation contribution, which was previously estimated using a coefficient of 1.5 W/m^2, whereas the model in this paper incorporates an analytical approach based on emissivity

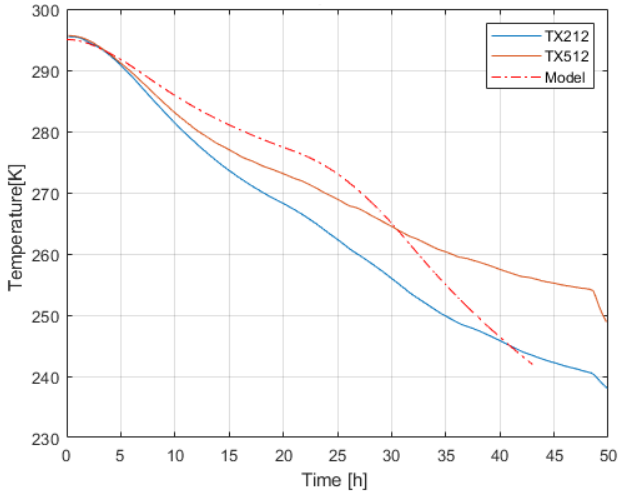

Figure 11: G11 support posts results.

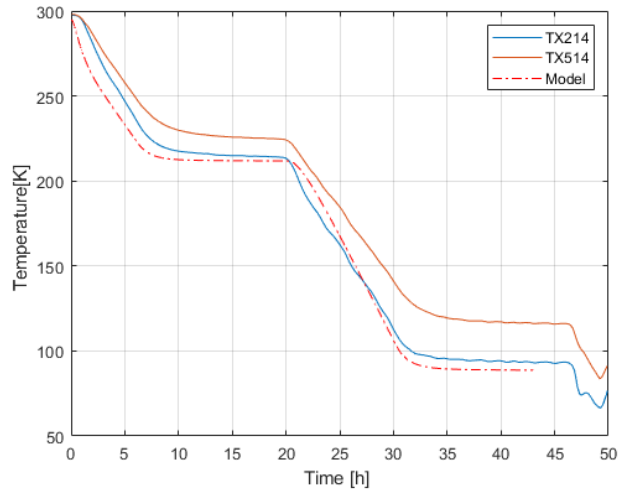

Figure 12: Cavity supports results.

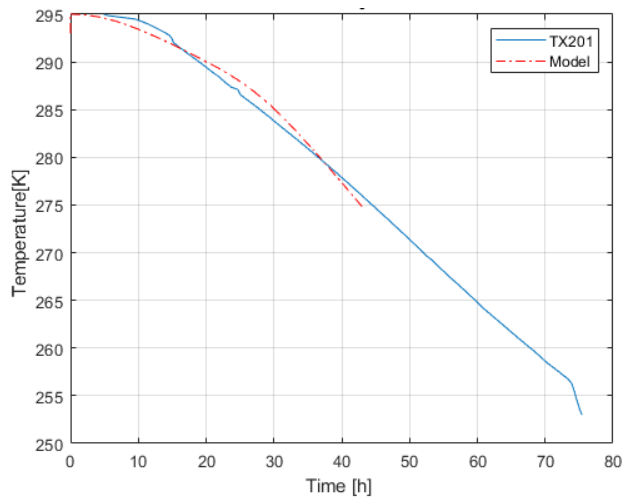

Figure 13: Cavity results.

coefficients and view factors. Regarding the heat loads on the LTTS and 2 K components, the previous calculations included additional losses such as those from view ports, PT lines, and beam lines, leading to higher overall heat loads. There is an important discrepancy with the heat loads measured during the first cool-down of the prototype

ISBN: 978-3-95450-234-9 ISSN: 2673-5504 doi:10.18429/JACoW-SRF2023-WEPWB073

cryomodule (see Table 1). However, the heat loads analysis of the first cool-down has identified addition heat sources that explain this discrepancy. These additional heat loads due to some MLI missing, microphonics in the cool down valve, and "Rollin film" within the cryogenic lines couldn't be modelled with Simulink/Simscape. Improvements are now ongoing to fix these issues and then cool-down again the cryomodule to validate the heat loads analysis [3].

Table 1: Static Heat Loads

	First estimated heat loads	Heat loads calculated with the model	Measured heat loads
High temperature thermal shield (HTTS)	150 W	163 W	250 W
Low temperature thermal source (LTTS)	26 W	25 W	30 W
2 K	11.2 W	10.6 W	52 W

ACKNOWLEDGMENT

The authors would like to thank the cryogenic team in charge of cooling down and operating the cryomodule.

CONCLUSION

The Simulink/Simscape model of the prototype HB650 cryomodule is validated. The transient analysis matches with the model predictions, and the heat loads during operation at 2 K issued from the model match the heat loads estimated with analytical calculations.

The next step is to continue optimizing this model with the second cool down of this prototype cryomodule and then to transpose this work to the SSR1, SSR2, and LB650 cryomodules.

REFERENCES

[1] E. Pozdeyev, "High power proton sources for neutrino science", presented at IPAC'21, Campinas, SP, Brazil, May 2021, paper THXX02, unpublished.

[2] V. Roger *et al.,* "Design of the 650 MHz high beta prototype cryomodule for PIP-II at Fermilab", in *Proc. SRF'21*, Michigan State University, USA, Jun.-Jul. 2021, pp. 671-675 doi:10.18429/JACoW-SRF2021-WEPTEV015

[3] V. Roger *et al*., "HB650 cryomodule design: from prototype to production", presented at *SRF'23*, Grand Rapids, MI, USA, Jun. 2023, paper WEPWB067, this conference.

[4] C. Lhomme *et al*., "An approach for component-level analysis of cryogenic process in superconducting linac cryomodules", in *Proc. LINAC'22*, Liverpool, UK, Aug. 2022, pp. 487-490. doi:10.18429/JACoW-LINAC2022-TUPOGE04

[5] N. Bazin *et al.,* "Design of the PIP-II 650 MHz low beta cryomodule", in *Proc. SRF'21*, East Lansing, MI, USA, Jun.-Jul. 2021, pp.841-844. doi:10.18429/JACoW-SRF2021-THPTEV006

[6] J. Bernardini *et al*., "Final design of the pre-production SSR2 cryomodule for PIP-II project at Fermilab", in *Proc SRF'21*, East Lansing, MI, USA, Jun.-Jul. 2021, pp.511-514. doi:10.18429/JACoW-SRF2021-TUPOGE12

[7] J. Bernardini *et al*., "Final design of the production SSR1 cryomodule for PIP-II project at Fermilab", presented at *SRF'23*, Grand Rapids, MI, USA, Jun. 2023, paper WEPWB066, this conference.

[8] V. Roger *et al*., "Design strategy of the PIP-II cryomodules", in *Proc SRF'19*, Dresden, Germany, Jun. 2019, pp. 307-310. doi:10.18429/JACoW-SRF2019-MOP094

[9] V. Roger *et al*., "Standardization and first lessons learned of the prototype HB650 cryomodule for PIP-II at Fermilab", in *Proc LINAC'22*, Liverpool, UK, Aug. 2022, pp. 526-528. doi:10.18429/JACoW-LINAC2022-TUPOGE16